Adsorption structure of cyclopentene on InP(001)(2×4)

Regina Passmann,[1,2,*] Priscila Favero,[3] Wolf Gero Schmidt,[4] Ronei Miotto,[5] Walter Braun,[6] Wolfgang Richter,[7,1] Michael Kneissl,[1] Norbert Esser,[1,2] and Patrick Vogt[1]

[1]*Institut für Festkörperphysik, Technische Universität Berlin, Hardenbergstr. 36, D-10623 Berlin, Germany*

[2]*ISAS–Institute for Analytical Sciences Department Berlin, Albert-Einstein-Str. 9, 12489 Berlin, Germany*

[3]*Instituto de Física da Universidade de Brasília, Caixa Postal 04455, CEP 70919-970 Brasília, DF, Brazil*

[4]*Universität Paderborn, Warburger Str. 100, 33098 Paderborn, Germany*

[5]*Centro de Ciências Naturais e Humanas, Universidade Federal do ABC, Rua Santa Adélia 166, CEP 09210-170 Santo André, SP, Brazil*

[6]*Helmholtz-Zentrum Berlin für Materialien und Energie, Elektronenspeicherring BESSY II, Albert-Einstein-Str. 15, 12489 Berlin, Germany*

[7]*Universita degli Studi Roma "Tor Vergata," Via della Ricerca Scientifica 1, 00133 Roma, Italy*

(Received 3 September 2008; revised manuscript received 29 March 2009; published 9 September 2009)

We have studied the interface formation between cyclopentene and (2×4) reconstructed InP (001) surfaces by soft x-ray photoemission spectroscopy, reflectance anisotropy spectroscopy (RAS), and *ab initio* theory. After preparation of an uncontaminated (2×4) reconstruction under ultrahigh vacuum conditions, the surface was exposed to cyclopentene as monitored by RAS. The changes in the In 4*d*, P 2*p*, and C 1*s* core-level emission lines upon molecule adsorption indicate a covalent bonding of cyclopentene to the topmost atoms of the surface at two different bonding sites. Based on these results, a structure model is suggested, which is supported by *ab initio* calculations of the total-energy, the RAS signature, and the In 4*d* and P 2*p* core-level shifts. Our results suggest that the cyclopentene adsorption is a two-step process: first cyclopentene adsorbs on the "mixed dimer" and second the changes in the surface structure enable the additional adsorption on the second layer In–In surface bond.

DOI: 10.1103/PhysRevB.80.125303 PACS number(s): 61.66.Hq, 72.80.Le, 68.47.Fg

I. INTRODUCTION

Hybrid systems consisting of thin organic layers and inorganic semiconductor surfaces are considered a key issue for future developments in the field of advanced electronic devices and sensors with a possible impact in many research areas such as biotechnology, nanoelectronics, high-density data storage, and medical diagnostics. The enormous variety of organic molecules in terms of structure and functionality enables novel applications by modification of semiconductor surfaces.[1–3] For these applications, the role of the interface formation and the related interfacial electronic properties are crucial. Bonding sites and bonding configuration of the organic molecules will influence the functionality of such a modified surface, for example, the translation of a surface reaction into a measurable signal, as well as the interface stability.[4] Therefore, a detailed knowledge of the atomic structure and the electronic properties of the interface bonds is required. So far, most of the results on hybrid interfaces are reported for the adsorption of organic molecules on Si(001) surfaces (for example, Refs. 1, 2, and 5–9). One of the most investigated surfaces is the Si(001)(2×1) surface, which is well understood and described by asymmetric buckled surface Si–Si dimers[10] forming local $p(2\times2)$ and $c(2\times4)$ arrangements. It was shown that for the adsorption of small organic ring molecules via a [2+2] cycloaddition reaction, the asymmetric dimer configuration is a basic prerequisite.[2,11] For the adsorption of organic molecules on surfaces of the technologically important III–V semiconductor surfaces, on the other hand, only little is known.[12–16] However, the combination of organic molecules and III–V semiconductor materials offers an ideal platform for applications in the field of electronic and optoelectronic devices.

In this paper, we report on the adsorption of cyclopentene on the InP(001)(2×4) reconstructed surface. The atomic structure of InP(001)(2×4) surface has been addressed in recent years and is explained by the "mixed-dimer" model, a structure that consists of a In-P heterodimer with a filled dangling bond at the P atom and an empty dangling bond at the In atom.[17,18] These dimer atoms are bonded to fourfold-coordinated second layer In atoms. The outer In atoms of the second layer are threefold coordinated and have empty dangling bonds. The resulting structure configuration is shown in Fig. 1 on the left.

Core-level spectroscopy and reflectance anisotropy spectroscopy (RAS) were performed to investigate the interface formation between InP(001)(2×4) and cyclopentene. Nu-

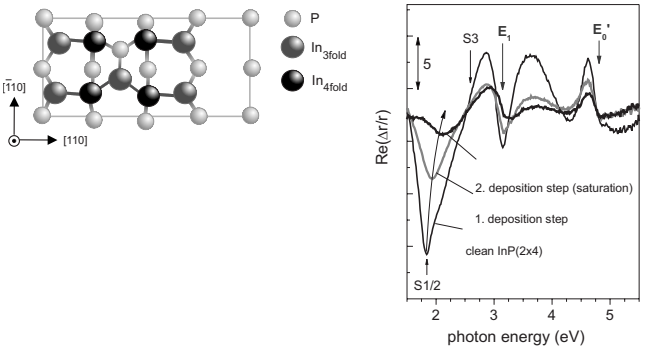

FIG. 1. On the left: topview of the InP(001)(2×4) surface reconstruction. On the right: RAS spectra $[\mathrm{Re}(r_{[-110]}-r_{[110]}/\langle r\rangle)\times10^{-3}]$ taken during the deposition of cyclopentene on InP(001)(2×4).

merical analysis of the In $4d$, P $2p$, and C $1s$ core-level emission lines by best fit reveals information on the surface bonding sites and chemical characteristics of the molecule adsorption. RAS was used to investigate the interface formation *in situ* as a monitoring tool. This surface sensitive optical technique can be applied for the characterization of the interface optical and electronic properties.[19] Based on the experimental results, structure models for the molecule-surface linkage were developed and compared to *ab initio* calculations of the total energy, the optical anisotropy, and the core-level shifts. Such a combination of experimental and theoretical techniques has been proven to be a powerful tool for the determination of surface structural and electronic properties, for example, for the clean InP(001)(2×1) and InP(001)(2×4) reconstructions.[17,18,20]

II. EXPERIMENTAL

The Sb-doped InP(001) samples investigated here were grown by metal-organic vapor phase epitaxy (MOVPE) using phosphine (PH_3) and trimethylindium as precursors. Directly after growth the samples were capped with an amorphous phosphorous/arsenic double layer by photodecomposition of PH_3 and AsH_3 in the MOVPE reactor.[21] After the transfer of the InP samples to UHV, contamination-free and well-ordered (001) surfaces were prepared by successive annealing for 15 min to approximately 400 °C (±20 °C). In order to obtain reproducibly well-ordered surfaces, the whole preparation process was monitored by quadrupole mass spectrometry and RAS. The RAS setup used here operates at nearly normal incidence in a photon energy range from 1.5 to 5.5 eV. The measurements were performed with the light polarized along the [110] and the $[\bar{1}10]$ directions of the sample. More details of the RAS setup are described in Ref. 22. The InP(001) surface reconstruction was determined by low-energy electron diffraction (LEED) showing a clear (2×4) pattern. The base pressure throughout all experiments was below 2×10^{-10} mbar.

Cyclopentene with a purity better than 97% was introduced into the chamber using a variable gas-inlet valve. During the deposition, the InP(001)(2×4) samples were held at room temperature. In order to avoid decomposition of the molecules, all filaments inside the chamber, e.g., ion gauges, were switched off during exposure. The effective cyclopentene layer thickness was estimated from soft x-ray photoemission spectroscopy (SXPS) measurements and determined to be approximately one monolayer. The whole deposition process was monitored by RAS.

Synchrotron-based photoemission measurements were performed at the Russian-German beamline at the synchrotron facility BESSY II. The spectra were taken in normal emission with a total instrumental resolution (beamline plus analyzer) determined to be 120 meV at an excitation energy of 75 eV (accounting for the energy range of In $4d$ and P $2p$). For the measurement of the C $1s$ core level, a higher excitation energy of around 320 eV is necessary with an instrumental resolution determined to be approximately 220 meV.

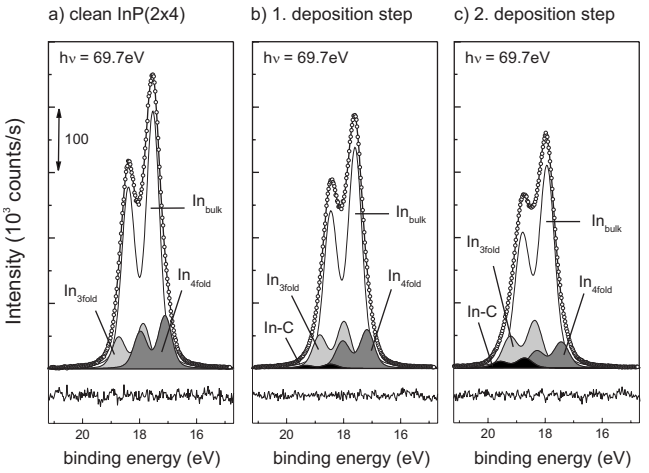

FIG. 2. The In $4d$ core level for the clean (left), for the partly cyclopentene covered (middle), and cyclopentene saturated (right) InP(001)(2×4) reconstructed surfaces.

The analysis of experimental core-level spectra is performed by fitting the experimentally determined peak shape with a theoretical model curve based on the nonlinear least-squares curve-fitting algorithm of Marquardt.[23] The theoretical curve is assembled from contributions of the core electrons as well as a background or baseline curve. The background signal, resulting from inelastically scattered electrons, is fitted with a polynomial of third order. Spin-orbit split doublets for In $4d$ and P $2p$ and single peaks for C $1s$ with a Lorentzian and Gaussian broadening were convoluted (Voigt profile) to simulate the measured line shape of the core level. The Lorentzian line shape accounts for the natural broadening mostly due to the lifetime of the core hole, whereas the Gaussian broadening includes the instrumental resolution and any broadening due to surface-potential variations and sample inhomogeneities. The scope of the fitting was to obtain a residuum (difference between fit and the measured data) without structures exceeding the noise level for a minimum number of shifted components. The residuum is thus a measure of the accuracy of the fit and is shown beneath each spectrum.

The spectra for the P $2p$, In $4d$, and C $1s$ emission were taken at photon energies (kinetic energies), which are in the range of kinetic energies of minimum electron mean free path for the maximum surface sensitivity. The binding energies of the core level given in the plots are referred to the Fermi edge (E_F) of a metal in electric contact with the InP sample. The spectra (dotted lines in Fig. 2–4) are shown together with best fit from the numerical analysis (straight lines). For all measurements, a lifetime broadening for the In $4d$ and P $2p$ core levels of 0.1 and 0.06 eV, a branching ratio of 1.5 and 2.0, an experimental broadening of 0.46 and 0.41 eV, and a spin-orbit splitting of 0.86 and 0.87 eV were found, respectively. These values are in good agreement with previously published results.[24] For the C $1s$ core level, a lifetime broadening 0.1 eV and an experimental broadening around 1.0 eV were obtained, which are in good agreement with results obtained after cyclopentene adsorption on Si(001).[25]

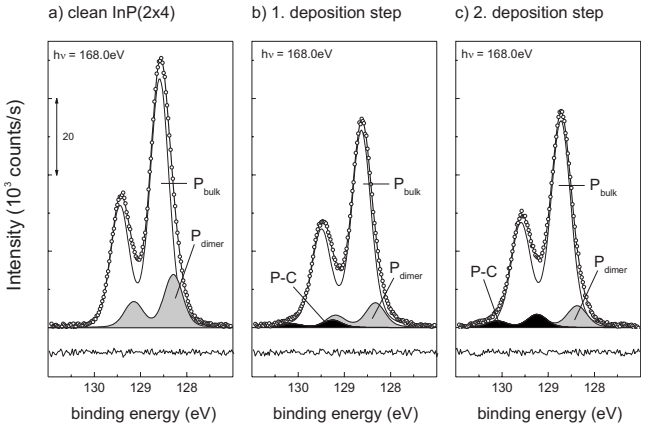

FIG. 3. The P $2p$ core level for the clean (left), for the partly cyclopentene covered (middle), and cyclopentene saturated (right) InP(001)(2×4) reconstructed surfaces.

III. THEORETICAL MODELING

Our calculations are based on the density-functional theory (DFT) as implemented in the Vienna *ab initio* simulation package (VASP).[26] In detail, the surface was modeled in a supercell geometry, with an atomic slab of nine layers and a vacuum region equivalent to seven atomic layers. All surface calculations were performed at the calculated equilibrium lattice constant of InP of 2.57 Å, which is in good agreement with the experimental findings of 2.54 Å.[27]

The cyclopentene molecules were placed on the top side of the slab, whereas the bottom side was passivated by pseudohydrogen arranged in a dihydride structure. The calculations for cyclopentene in the gas phase were made using a cubic unit cell with a lattice constant of 15 Å. The electron-ion interaction is described by projector augmented wave potentials[28,29] and the electron-electron exchange-correlation interactions were simulated using the generalized gradient approximation.[30] The single-particle orbitals were expressed in a plane-wave basis up to the kinetic energy of 450 eV. For the Brillouin-zone summation, 10 (770) and 4 (16) special **k** points were used for electronic structure (optical response) calculations for the bulk and surface, respectively. The atoms were assumed to be in their fully relaxed positions when the forces acting on the ions were smaller than 0.01 eV/Å. The adsorption energy is obtained from the difference between the total energy for the analyzed configuration and the energy for the free InP(001)(2×4) surface plus the total energy for a cyclopentene molecule in the gas phase. The reflectance anisotropy is calculated from

$$\frac{\Delta r}{r}(\omega) = \frac{(2\omega d)}{c}\mathrm{Im}\frac{\epsilon_{110}^{slab}(\omega) - \epsilon_{1\bar{1}0}^{slab}(\omega)}{\epsilon_b(\omega) - 1}, \quad (1)$$

where $\epsilon_b(\omega)$ is the bulk dielectric function and $\epsilon_{110}^{slab}(\omega)$ and $\epsilon_{1\bar{1}0}^{slab}(\omega)$ are the respective components of the surface dielectric function.[31,32] Core-level shifts are calculated following the theoretical approach suggested by Köhler and Kresse.[33] It is important to note that this theoretical approach is not able to provide absolute core binding-energy values but only relative shifts.[33]

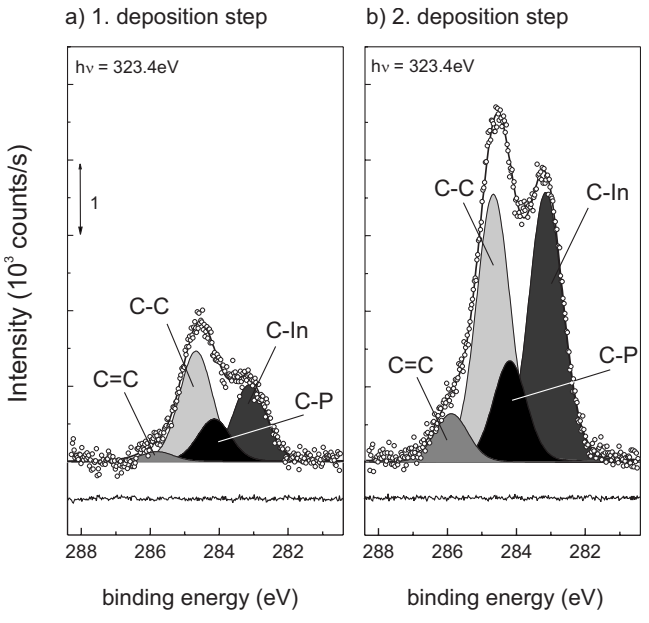

FIG. 4. The C 1s core level for the partly cyclopentene covered (left) and cyclopentene saturated (right) InP(001)(2×4) reconstructed surfaces.

IV. RESULTS AND DISCUSSION

A. Experimental results

In Fig. 1 (right side), the evolution of the RAS signature upon deposition of the cyclopentene molecules on the InP(001)(2×4) is depicted. The RAS spectrum of the clean InP surface (thin line) exhibits at lower photon energies three features named S_1, S_2, and S_3, which originate from surface states located in the uppermost atomic layers.[17] It can clearly be seen that upon adsorption of cyclopentene, changes at these surface related features occur. The deposition was carried on until no further changes in the RAS line shape could be seen. This point is defined as saturation and refers to a deposition of roughly one monolayer determined by the SXPS intensity attenuation. As the RAS setup is limited to photon energies between 1.5 and 5.5 eV, no molecular transitions can be observed. During the deposition, the (2×4) LEED pattern of the clean surface vanishes.

Chemical information on the bonding configuration of the cyclopentene molecules is derived from the SXPS measurements. In Figs. 2(a) and 3(a), measurements of the In 4d and P 2p core levels for the initial InP(001) (2×4) surface are displayed measured at an excitation energy of 69.7 eV and 168.0 eV, respectively. For the In 4d emission line, two additional surface components (shaded) are revealed by numerical analysis within the spectrum shifted by −0.45 eV toward lower binding energies and +0.38 eV toward higher binding energies with respect to the bulk component. For the P 2p core level, one surface component (P_{dimer}) with a lower binding-energy shift of −0.31 eV shows up. These results are in agreement with previous publications apart from slight differences of the energy shift values due to better spectral

resolution in the present case.[18] The surface components are well explained within the mixed-dimer model.[18] The surface component of the P $2p$ core level stems from the mixed In–P dimer in the outermost layer. The two surface components (low and high binding energies) of In $4d$ refer to the two inequivalent group-III sites in the surface unit cell (see Fig. 1 on the left). The high binding-energy component (In_{3fold}) is associated with charge depletion with respect to the bulk, corresponding to sites with an empty dangling bond (threefold coordination). This holds for the III site of the mixed dimer and for another four sites per unit mesh in the second layer. The remaining four sites in the second layer, right beneath the mixed dimer, are associated with charge accumulation with respect to the bulk since also bonds between group-III atoms (III-III bonds) occur within the fourfold coordination of these sites [In_{4fold} (see Fig. 1 on the left)].

During the deposition of cyclopentene the In $4d$ core level, emission line shape is modified [Figs. 2(b) and 2(c)]. The In_{4fold} component decreases clearly, whereas the second surface component In_{3fold} increases slightly up to the saturation level. Additionally, a new surface component labeled In–C is obtained by numerical analysis shifted by +0.84 eV toward higher binding energies. This component is assigned to indium atoms, which bond to carbon atoms of the cyclopentene molecule. The shift toward higher binding energies results from a charge transfer from In (1.78) to C (2.55) due to the higher electronegativity of the latter. The In-C component increases until saturation as expected. Also in the case of the P $2p$ core level depicted in Figs. 3(b) and 3(c), a new component (P–C) appears for both the partly covered and the saturated surface which is shifted by +0.59 eV toward higher binding energies. Due to the lower electronegativity of phosphorus (2.19) compared to carbon (2.55), this component is associated to P atoms, which bond to C atoms of cyclopentene.

In Fig. 4, the corresponding C $1s$ core levels are shown recorded at an excitation energy of 323.4 eV. From the observed experimental line shape, it is immediately obvious that at least three different contributions can be distinguished: two maxima and a shoulder at higher binding energies. However, the numerical analysis with only three components did not result in a satisfying agreement with the experimental results, meaning that the residuum would always show structure clearly above the noise level independently of the experimental broadening. This is a clear indication for an additional component contributing to the core-level emission line. Using four components, the numerical analysis revealed for both deposition steps flat residuals with variations only within the noise level. For five and more components, the quality of the fit could not further be improved showing that only four components should be used for the analysis. The main most intense component is assigned to stem from carbon atoms involved in C–C single bonds within the cyclopentene molecule. The two other strong components are shifted by −1.4 eV (C–In) and −0.50 eV (C–P) toward lower binging energies with respect to the C–C component. Corresponding to the In $4d$ and P $2p$ results, these two C $1s$ components are assigned to the carbon atoms involved in C–In and C–P bonds, respectively. The energetic shifts are in agreement with the different electronegativity values of phosphorus (2.19), indium (1.78), and carbon (2.55), meaning that the C–P and C–In components are shifted to lower binding energies with respect to the C–C component and the energetic shift of C–In is larger than the one of C–P. The fourth small component is shifted by +1.17 eV toward higher binding energies with respect to the C–C component and is assigned to carbon atoms participating in C=C double bonds of cyclopentene. Similar to results reported for the adsorption of cyclopentene on $Si(001)(2\times1)$,[25] we conclude that this component results from additional physisorbed cyclopentene molecules. This is reasonable since this component is rather small with respect to the others. The core-level results unambiguously show that the main adsorption of cyclopentene on the $InP(001)(2\times4)$ surface takes place between the mixed In–P dimer and the two carbon atoms involved in the C=C double bond of cyclopentene. During the adsorption, the C=C double bond breaks and is transformed into a C–C single bond and the C atoms form bonds to the In and P atoms of the In–P surface dimer. Such a bonding configuration explains all the observed new core-level components of the participating atoms. However, it is obvious in Fig. 4 that between the two deposition steps not only the intensity but the line shape of the C $1s$ core-level emission changes. This is a result of the relative increase in the C–In component with respect to the others, in particular, the C–P component. Such a line-shape change is a clear evidence for a second bonding site on the surface. At the same time, it was observed that the In_{4fold} component of the In $4d$ decreases more strongly, while the In_{3fold} increase is smaller for the second deposition step [in Fig. 2(c)].

These findings suggest that the surface exhibits a second adsorption site in the second In-terminated layer. This means that now more In atoms than P atoms are involved in the bond formation to cyclopentene, which leads to an increase in the C $1s$ C–In component with respect to the C–P component. Due to this evolution of the C $1s$ line shape with the deposition, it can also be concluded that the second bonding site is only possible if a cyclopentene molecule is already bond to the mixed In–P top dimer. The most likely bonding configuration to explain these results is on top of the second layer In–In dimmers, which consist of In atoms with a threefold and fourfold coordinations. As a result of this bonding, the In_{4fold} component decreases more strongly with the second deposition step. However, for the bonding on the In–In dimers a new In $4d$ component would be expected, which is not necessary for the numerical analysis of the In $4d$ core-level emission, meaning that the residual cannot further be improved. This can be explained by the limited experimental resolution since this new component is expected to be found between the In_{3fold} and the In–C components. Nonetheless, a more indirect indication for such an additional component is given by the fact that the Gaussian broadening of the In $4d$ components increases between the first and the second deposition steps by approximately 60 meV (from 460 to 520 meV). However, since this difference is obviously below the resolution limit of 120 meV, it is no clear proof for the additional component.

After adsorption of the cyclopentene molecules on the InP(001) surface, it is possible to restore the initial (2×4)

reconstruction by thermal desorption of cyclopentene (not shown here). By heating the samples to approximately 430 °C(±20 °C) for 15 min, the LEED pattern shows again a (2×4) surface symmetry and the RAS line shape looks similar to the one obtained at the initial clean InP(001)(2×4) surface. SXPS measurements show that the C 1*s* has vanished and the In 4*d* and P 2*p* core-level emissions show the core-level shifts of the clean InP(001)(2×4) surface. This means that cyclopentene is fully desorbed from the surface. The desorption temperature is much lower compared to desorption of cyclopentene from the Si(001)(2×1) surface, where a heating temperature around 900 °C is required, indicating that the binding energy of cyclopentene on the InP(001)(2×4) must be clearly smaller than that for the Si surface.

B. Theoretical results

In order to further elucidate the bonding configuration of cyclopentene on the InP(001)(2×4) surface, including the different bonding sites, bonding configuration and possible dissociation of cyclopentene, *ab initio* calculations including full structural relaxations were performed. The results are presented in this section. Our present results for the clean InP surface agree with previous studies,[17,18] indicating an In–P heterodimer with a filled dangling bond at the P atom and an empty dangling bond at the In atom. The asymmetric dimer bond length for the In–P bond is 2.6 (2.44) Å with a vertical buckling of 0.52 (0.46) Å. The cyclopentene interaction with the InP(001)(2×4) surface is investigated by considering a series of possible adsorption configurations, which include (a) bonding on top of the In–P mixed dimer, (b) single bond configuration of the molecule, and (c) bonding on the second layer In–In dimers (parallel and perpendicular to it). For the first case, different subarrangements are considered, including cis-type (hydrogen at the same side of the molecule), trans-type (hydrogen at alternating sides of the molecule), dissociated (hydrogen is dissociated and transferred to mixed-dimer atoms), dimer-cleaved (the In–P dimer breaks), and dimerized (the In–P dimer remains intact) configurations. A selection of the considered bonding arrangements is illustrated in Fig. 5. Among all studied configurations, only the cis-type dimerized configuration is found to be exothermic, i.e., the adsorbed system is lower in energy compared to the constituents.

The adsorption of cyclopentene on top of the intact mixed dimer is the energetically most favored geometry. The alternative dimer-cleaved model was tested by considering an increasing in the dimer bond length and a possible adsorption of H on the mixed dimer. In both cases, the TE calculations indicate that these configurations are energetically not favorable since their calculated energies are higher than those obtained by the bare InP surface and the free cyclopentene molecule by more than 0.15 eV. In a similar manner, the trans-type dimer-cleaved structure, the cis-type, and the trans-type adsorption on In–In dimer are found to be less stable than the bare InP surface and the free cyclopentene molecule by 0.09, 0.15, and 0.16 eV, respectively.

The adsorption energy for the cis-type dimerized configuration is determined to be −0.28 eV, which is in good agreement with the heating experiments described above. It is much smaller than the about −1.2 eV obtained by various authors[2,34–36] for the adsorption of cyclopentene on the silicon surface. Upon cyclopentene adsorption, the buckling of the mixed dimer changes into the opposite direction and decreases by 0.53 Å, whereas the second layer In–In dimer buckling increases by 0.43 Å. This dimer rearrangement suggests a charge transfer between In and P atoms in analogy to the Si–Si dimer tilting of the bare silicon surface. Indeed, a comparison of the second highest-occupied molecular state from the bare InP surface and the adsorbed system (not shown here) clearly indicates a charge redistribution due to the interaction between cyclopentene and the surface.

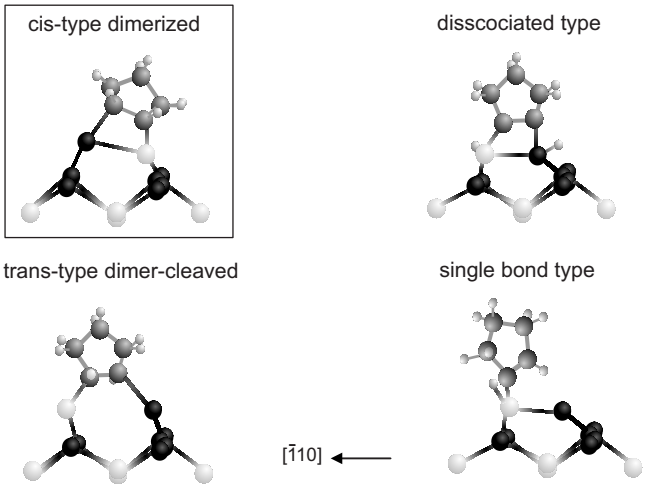

FIG. 5. Schematic representation of possible adsorption structures of cyclopentene at the mixed dimer of the InP(001)(2×4). Only the cis-type dimerized model is found to be energetically stable.

To further support the cis-type dimerized model for the cyclopentene adsorption on InP(001)(2×4), we also calculated the optical anisotropy and the core-level shifts for In 4*d*. To determine the influence on the optical anisotropy, the RAS changes caused by cyclopentene adsorption were calculated. The calculation of the difference of the RAS signals of clean and cyclopentene adsorbed surface leads to a cancellation of numerical artifacts related to the slab bottom atoms. Similarly, one can calculate the difference of the measured signals before and after adsorption of cyclopentene. The comparison of experimental and calculated spectrum in Fig. 6 indicates that the energetically most favorable cis-type dimerized structure accounts qualitatively for the experimentally observed optical anisotropy. The calculated RAS difference spectrum for the model with the two adsorption sites is also presented in Fig. 6 (thick line, lower graph) and shows only small differences to the one for the cis-type dimerized model (thin line, lower graph) and is also in agreement with the experimental one (upper graph).

Despite the qualitative agreement, it can be seen that the experimental results are blueshifted by 0.35 eV in comparison with the calculated ones. The reason is that DFT calculations do not take electronic self-energy effects into account (see, e.g., Ref. 37) and thus underestimate the band-gap

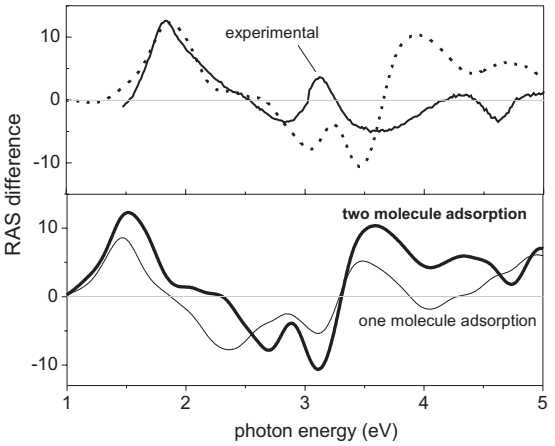

FIG. 6. RAS difference spectra obtained from the difference between the RAS signals from cyclopentene modified and the clean reconstructed surface. Depicted are the calculated difference spectrum for the adsorption of one (thin line, lower graph) and two (thick line, lower graph) cyclopentene molecules per surface unit cell as well as the experimental spectra (upper graph). In the upper graph, the calculated difference spectra of the two molecule adsorption shifted by 0.35 eV are shown (dashed line) for a better comparison together with the experimental data.

energies of semiconductors typically by up to 50%. From the theoretical spectra, we determine the E_1 and E_0' peaks of the InP bulk optical spectrum around 2.4 eV $\pm$ 0.2 eV and 4.2 eV $\pm$ 0.2 eV. Experimentally, (see Fig. 1) they are observed at 3.2 and 4.8 eV, in agreement with previous results.[38]

The (energy-dependent) self-energies, which—on the other hand—dependent on the excitation energies, are small around the Fermi energy. Therefore, a rigid shift is only an approximate "cure" for the DFT band-gap problem. However, for a better comparison to the experimental spectrum, we have also shown the calculated RAS spectrum shifted by 0.35 eV (dashed line) in Fig. 6. It is important to mention that both RAS spectra are calculated for ideal fully covered surfaces with perfect (2×4) translational symmetry, which is obviously not the case in the experiment.

The core-level shifts were calculated following the approach suggested by Köhler and Kresse.[33] Assuming that the bottom In atoms approximate well bulk material, we found for the initial InP(001)(2×4) reconstruction two different In 4*d* surface core-level components shifted by −0.48 and +0.42 eV toward lower and higher binding energies, which are in good agreement with the experimentally determined shifts of −0.45 and +0.38 eV. After the adsorption of cyclopentene and the covalent bond formation to the mixed In–P dimer, the induced In 4*d* core-level component is shifted by +0.65 eV toward higher binding energies. This value is consistent with the new experimentally observed In–C component shifted by +0.84 eV.

Motivated by the SXPS results, the theoretical investigations were extended toward a second possible cyclopentene adsorption site on the next layer In–In dimers. The TE calculation shows that this adsorption configuration is an energetically favorable process with an adsorption energy of −0.1 eV. Although a second molecule adsorption does not result in the lowest-energy configuration, it is interesting to emphasize that the adsorption on a In–In dimer within a surface unit cell is only possible after a previous adsorption of cyclopentene on the neighboring mixed dimer, which is consistent with the interpretation of the C 1*s* core-level evolution upon deposition. The corresponding structure model is depicted in Fig. 7.

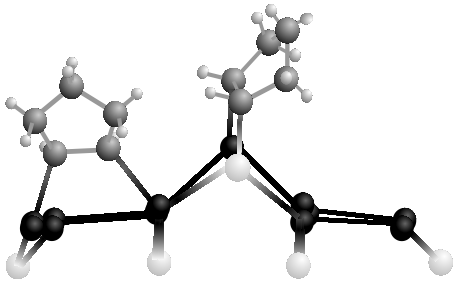

FIG. 7. Schematic representation of the adsorption of cyclopentene at the mixed dimer and at an additional second adsorption site on the second layer In–In bonds of the InP(001)(2×4) surface.

The calculated In 4*d* core-level shift for bonding on the second layer In–In dimers amounts to +0.72 eV, which is very close to the one for the adsorption on the top In–P dimer of (+0.65 eV). Since these two shifts present a small energy difference, it was not possible to resolve them in the SXPS experiments mainly due to the limited experimental resolution.

It should be noted that, particularly in the case of two bonding sites, the cyclopentene molecules in two adjacent surface unit cells could be placed very close to each other and possibly interact either repulsively or attractively and thus influence the binding energy. To investigate such an influence, we have also determined the adsorption energies for cyclopentene molecules placed in a larger supercell by doubling the (2×4) in the $[\bar{1}10]$ direction, i.e., within a (4×4) surface unit cell. We have then considered three different adsorption scenarios. (a) For the adsorption of a single molecule on a cis-type dimerized configuration, an adsorption energy of 0.29 eV is obtained. If a second adsorption on the neighboring In–In dimers is considered, i.e., in the same (2×4) subunit, their absorption energy is determined to be 0.11 eV. Both values are very similar as for the above-described adsorption on the (2×4). (b) If the second molecule is placed in the second (2×4) subunit of the (4×4), the adsorption energy is negative meaning that the molecule desorbs again. This result is consistent with the results explained above, which show that the adsorption on the In–In dimers is only possible if a cyclopentene molecule is already adsorbed on the adjacent In–P dimer. (c) If two molecules are placed on the 2 In–P mixed dimers of the (4×4), an adsorption energy for each molecule of 0.26 eV is obtained, which is 0.02 eV below the calculated value for the (2×4) surface.

Thus, it can be concluded that by doubling the surface unit cell, i.e., considering a (4×4), no noticeable changes are observed concerning the adsorption energies and the atomic or electronic structures calculated upon adsorption of cyclopentene on InP(001). This means that for the adsorption

of cyclopentene on InP(001)(2×4), the intermolecular interaction between the adsorbed molecules can be neglected.

V. SUMMARY

In conclusion, we have shown that by combining RAS and SXPS measurements as well as first-principles calculations, the adsorption of cyclopentene on the mixed-dimer InP(001)(2×4) surface can be understood in the following way: the first adsorption takes place on the In–In heterodimer in the cis-type dimerized geometry followed by the adsorption of a second cyclopentene molecule on the second layer In–In dimer, as shown in Fig. 7. Adsorption on the In–In dimer, however, is only possible after a cyclopentene molecule is adsorbed on the adjacent top In–P dimer.

ACKNOWLEDGMENTS

We would like to thank S. Weeke and M. Pristovsek for the growth of the InP substrates. We would also like to acknowledge financial support from the DAAD (Deutscher Akademischer Austauschdienst), VIGONI, the Deutsche Forschungsgemeinschaft and the Brazilian agencies FAPESP, CNPq, and CAPES.

*regina.passmann@gmx.de

[1] R. Hamers, Nature (London) **412**, 489 (2001).
[2] S. F. Bent, Surf. Sci. **500**, 879 (2002).
[3] Z. Liu, A. A. Yasseri, J. S. Lindsey, and D. F. Bocian, Science **302**, 1543 (2003).
[4] A. Vilan and D. Cahen, Trends Biotechnol. **20**, 22 (2002).
[5] J. S. Hovis, H. Liu, and R. J. Hamers, Surf. Sci. **402-404**, 1 (1998).
[6] J. W. Kim, M. Carbone, M. Tallarida, J. H. Dil, K. Horn, M. P. Casaletto, R. Flammini, and M. N. Piancastelli, Surf. Sci. **559**, 179 (2004).
[7] C. A. Hacker and R. J. Hamers, J. Phys. Chem. B **107**, 7689 (2003).
[8] A. Hermann, W. G. Schmidt, and F. Bechstedt, Phys. Rev. B **71**, 153311 (2005).
[9] W. G. Schmidt, F. Fuchs, A. Hermann, K. Seino, F. Bechstedt, R. Passmann, M. Wahl, M. Gensch, K. Hinrichs, N. Esser, S. Wang, W. Lu, and J. Bernholc, J. Phys.: Condens. Matter **16**, S4323 (2004).
[10] H. Q. Yang, C. X. Zhu, Z. Q. Xue, and S. J. Pang, Surf. Sci. **448**, 225 (2000).
[11] R. J. Hamers, J. S. Hovis, S. Lee, H. Liu, and J. Shan, J. Phys. Chem. B **101**, 1489 (1997).
[12] S. D. Silaghi and D. R. T. Zahn, Appl. Surf. Sci. **252**, 5462 (2006).
[13] T. U. Kampen, U. Rossow, M. Schumann, S. Park, and D. R. T. Zahn, J. Vac. Sci. Technol. B **18**, 2077 (2000).
[14] Y. Chen, J. Schmidt, L. Siller, J. C. Barnard, and R. E. Palmer, Phys. Rev. B **58**, 1177 (1998).
[15] T. Angot, E. Salomon, N. Papageorgiou, and J.-M. Leyet, Surf. Sci. **572**, 59 (2004).
[16] R. Passmann, M. Kropp, T. Bruhn, B. O. Fimland, F. L. Bloom, A. C. Gossard, W. Richter, N. Esser, and P. Vogt, Appl. Phys. A: Mater. Sci. Process. **87**, 469 (2007).
[17] W. G. Schmidt, N. Esser, A. M. Frisch, P. Vogt, J. Bernholc, F. Bechstedt, M. Zorn, T. Hannappel, S. Visbeck, F. Willig, and W. Richter, Phys. Rev. B **61**, R16335 (2000).
[18] W. G. Schmidt, F. Bechstedt, N. Esser, M. Pristovsek, Ch. Schultz, and W. Richter, Phys. Rev. B **57**, 14596 (1998).
[19] M. Zorn, T. Trepk, J. T. Zettler, B. Junno, C. Meyne, K. Knorr, T. Wethkamp, M. Klein, M. Miller, W. Richter, and L. Samuelson, Appl. Phys. A: Mater. Sci. Process. **65**, 333 (1997).
[20] W. G. Schmidt, P. H. Hahn, F. Bechstedt, N. Esser, P. Vogt, A. Wange, and W. Richter, Phys. Rev. Lett. **90**, 126101 (2003).
[21] K. Knorr, M. Pristovsek, U. Resch-Esser, N. Esser, M. Zorn, W. Richter, and J. Chryst, Growth **170**, 230 (1997).
[22] W. Richter, Philos. Trans. R. Soc. London, Ser. A **344**, 453 (1993).
[23] D. Marquardt, J. Soc. Ind. Appl. Math. **11**, 431 (1963).
[24] P. Vogt, K. Lüdge, M. Zorn, M. Pristovsek, W. Braun, W. Richter, and N. Esser, J. Vac. Sci. Technol. B **18**, 2210 (2000); P. Vogt, A. M. Frisch, Th. Hannappel, S. Visbeck, F. Willig, Ch. Jung, R. Follath, W. Braun, W. Richter, and N. Esser, Appl. Surf. Sci. **166**, 190 (2000).
[25] H. Liu and R. J. Hamers, Surf. Sci. **416**, 354 (1998).
[26] G. Kresse and J. Furthmüller, Comput. Mater. Sci. **6**, 15 (1996).
[27] F. Bechstedt and R. Enderlein, *Semiconductor Surfaces and Interfaces* (Akademie-Verlag, Berlin, 1988), and references therein.
[28] P. E. Blöchl, Phys. Rev. B **50**, 17953 (1994).
[29] G. Kresse and D. Joubert, Phys. Rev. B **59**, 1758 (1999).
[30] J. P. Perdew, K. Burke, and M. Ernzerhof, Phys. Rev. Lett. **77**, 3865 (1996).
[31] W. G. Schmidt and F. Bechstedt, Surf. Sci. **409**, 474 (1998).
[32] R. Del Sole, Solid State Commun. **37**, 537 (1981).
[33] L. Köhler and G. Kresse, Phys. Rev. B **70**, 165405 (2004).
[34] S. Y. Quek, J. B. Neaton, M. S. Hybertsen, E. Kaxiras, and S. G. Louie, Phys. Status Solidi B **243**, 2048 (2006).
[35] J.-H. Cho and L. Kleinman, Phys. Rev. B **64**, 235420 (2001).
[36] W. Lu, W. G. Schmidt, and J. Bernholc, Phys. Rev. B **68**, 115327 (2003).
[37] M. S. Hybertsen and S. G. Louie, Phys. Rev. B **34**, 5390 (1986).
[38] P. Lautenschlager, M. Garriga, and M. Cardona, Phys. Rev. B **36**, 4813 (1987).